International Journal of Radiation Oncology biology • physics

www.redjournal.org

Biology Contribution

Radiation-Induced Alterations in Mouse Brain Development Characterized by Magnetic Resonance Imaging

Lisa M. Gazdzinski, PhD,* Kyle Cormier, BSc,* Fred G. Lu, PhD,† Jason P. Lerch, PhD,*,‡ C. Shun Wong, MD,†,‡,§ and Brian J. Nieman, PhD*,‡

**Mouse Imaging Centre, Hospital for Sick Children, †Department of Radiation Oncology, Sunnybrook Health Sciences Centre, ‡Department of Medical Biophysics, University of Toronto, and §Department of Radiation Oncology, University of Toronto, Toronto, Canada*

Received Mar 1, 2012, and in revised form Jun 17, 2012. Accepted for publication Jun 20, 2012

Summary

Many childhood cancer survivors suffer from neurocognitive late effects following cranial radiation therapy. In this study, longitudinal magnetic resonance imaging was used to identify regions of the mouse brain where development is altered after irradiation at a young age. We produce a map and time course of the radiation-induced developmental changes by brain region and present a technique that will allow high-throughput evaluation of neuroanatomic late effects in mouse models under various treatment conditions.

Purpose: The purpose of this study was to identify regions of altered development in the mouse brain after cranial irradiation using longitudinal magnetic resonance imaging (MRI).
Methods and Materials: Female C57Bl/6 mice received a whole-brain radiation dose of 7 Gy at an infant-equivalent age of 2.5 weeks. MRI was performed before irradiation and at 3 time points following irradiation. Deformation-based morphometry was used to quantify volume and growth rate changes following irradiation.
Results: Widespread developmental deficits were observed in both white and gray matter regions following irradiation. Most of the affected brain regions suffered an initial volume deficit followed by growth at a normal rate, remaining smaller in irradiated brains compared with controls at all time points examined. The one exception was the olfactory bulb, which in addition to an early volume deficit, grew at a slower rate thereafter, resulting in a progressive volume deficit relative to controls. Immunohistochemical assessment revealed demyelination in white matter and loss of neural progenitor cells in the subgranular zone of the dentate gyrus and subventricular zone.
Conclusions: MRI can detect regional differences in neuroanatomy and brain growth after whole-brain irradiation in the developing mouse. Developmental deficits in neuroanatomy persist, or even progress, and may serve as useful markers of late effects in mouse models. The high-throughput evaluation of brain development enabled by these methods may allow testing of strategies to mitigate late effects after pediatric cranial irradiation. © 2012 Elsevier Inc.

Reprint requests to: Brian J. Nieman, PhD, Toronto Centre for Phenogenomics, Mouse Imaging Centre, 25 Orde St, Toronto, Ontario, Canada, M5T 3H7. Tel: (647) 837-5828; Fax: (647) 837-5832; E-mail: bjnieman@phenogenomics.ca

This study was conducted with the support of the Ontario Institute for Cancer Research through funding provided by the Government of Ontario and with funding from the Canadian Institutes of Health Research.

Conflict of interest: none.

Supplementary material can be found at www.redjournal.org.

Int J Radiation Oncol Biol Phys, Vol. 84, No. 5, pp. e631–e638, 2012
0360-3016/$ - see front matter
http://dx.doi.org/10.1016/j.ijrobp.2012.06.053

Introduction

Leukemia and central nervous system (CNS) tumors account for almost half of all childhood cancers (1). With 5-year survival rates approaching 80%, the long-term quality of life for childhood cancer survivors is a growing concern (2). Late effects—delayed side effects that appear months or years after treatment—can include neurocognitive, endocrine, and social dysfunctions that manifest as decreased IQ scores, seizures, or difficulties with memory and attention (3).

Cranial irradiation is an important part of leukemia and CNS cancer treatments that confers a survival benefit (4). However, cranial irradiation has also been identified as an important causative factor leading to late effects (5, 6). Recent studies have therefore used intensified chemotherapy with the goal of replacing or delaying radiation therapy (7). Although these strategies are showing success for some cancers, the standard of care for many childhood malignancies continues to include cranial irradiation.

Modified treatment protocols or post-treatment intervention strategies are needed to mitigate the late effects due to radiation treatment of pediatric patients. However, the mechanisms that produce these late effects remain only partly characterized. It is clear that the CNS response to radiation is a continuous and dynamic process (8). Acute and subacute effects are believed to be due to early blood-brain barrier disruption, edema, and transient demyelination and tend to be reversible. Late effects are more often irreversible and progressive. Loss of neurogenesis, vascular changes, demyelination, and inflammation are factors that may be involved in the pathogenesis of late effects (9). The neurogenic niches of the dentate gyrus and subventricular zone are known to be particularly sensitive to radiation (10), and a loss of white matter has been well documented (11). Nonetheless, a systematic mapping of radiosensitivity in the developing brain has not been performed. This information could lead to treatment protocols in which different brain regions are treated at different times according to their radiosensitivity and the urgency for local tumour control.

The aim of this work is to characterize regional radiation-induced developmental alterations in the mouse brain using noninvasive, longitudinal magnetic resonance imaging (MRI). We characterize radiation-sensitive brain regions on the basis of changes in volume and growth rate. These data provide a baseline that will enable future investigations of the mechanisms of radiation damage using mouse models of development.

Methods and Materials

Mice

C57Bl/6J mice (Toronto Centre for Phenogenomics in-house colony) were used for all experiments. Because human studies have observed that girls are more prone to long-term cognitive deficits following cranial irradiation than boys (6), only female mice were evaluated in this initial study. Animal experiments were approved by the Toronto Centre for Phenogenomics Animal Care Committee.

Cranial irradiation

Pups aged 2.5 weeks old received a 7-Gy dose of radiation to the whole brain using a Cs-137 source (Gamma Cell 40, MDS Nordion). Assuming a fractionation sensitivity of $\alpha/\beta \sim 2$ Gy, this single dose is equivalent to a 16-Gy dose separated into 2-Gy fractions as used for prophylactic treatment of acute lymphoblastic leukemia. The mice were anesthetized using ketamine (75 mg/kg) and xylazine (5 mg/kg) for the irradiation, and their bodies were shielded with lead. Control mice were positioned entirely beneath the shielding. The 2.5-week age for the irradiation was chosen to correspond in stage of brain development to the human infant, with 2 weeks of age in the mouse considered equivalent to birth in the human (12).

In vivo MR imaging

One cohort of mice (20 irradiated and 19 control) was imaged longitudinally. MRI was performed on a 7-T scanner (Varian Medical Systems) at postnatal day 14 (before irradiation) and after irradiation at 3.5, 6, and 9 weeks of age. Twenty-four hours before each imaging session, mice received 0.4 mmol per kg $MnCl_2$ intraperitoneally for contrast enhancement (13). The imaging protocol consisted of a 3-dimensional gradient echo sequence (125-μm isotropic resolution, repetition time = 100 msec, echo time = 4 msec, flip angle = 55°, field-of-view/scan time = 1.8 × 1.8 × 3.5 cm / 1 hour and 10 minutes for pups and 2.1 × 2.1 × 3.5 cm / 1 hour 35 minutes for adults).

Ex vivo MRI

A second cohort of mice (15 irradiated and 13 control) were euthanized at 6 weeks of age and imaged ex vivo. To prepare the brains for ex vivo imaging, the mice were anesthetized using ketamine (150 mg/kg) and xylazine (10 mg/kg) and perfused through the heart with 30 mL phosphate-buffered saline + 1 μL per mL heparin + 2 mM ProHance (Bracco Diagnostics) followed by 4% paraformaldehyde + 2 mM ProHance at a rate of 1 mL per min. The mice were decapitated, the skin and lower jaw were removed, and the brain in the skull was soaked overnight in 4% paraformaldehyde + 2 mM ProHance, then transferred to phosphate-buffered saline + 2 mM ProHance + 0.02% sodium azide until being imaged (1-2 weeks). Ex vivo imaging was performed using a 3-dimensional fast spin echo pulse sequence (56 μm isotropic resolution, repetition time = 2000 msec, effective echo time = 42 msec, echo spacing = 14 msec, echo train length = 6, scan time ~11.5 hr).

Image analysis

A registration-based image analysis was used to assess anatomic differences between irradiated and control brains (14). Ex vivo and in vivo images were analyzed separately but followed similar registration procedures. In each case, the images were registered together through a process of linear and nonlinear registration steps to yield an average image. The determinant of the Jacobian matrix for each image was computed, providing a measure of local volume change at every voxel in the brain for comparison between control and irradiated groups. A segmented anatomical atlas with 62 labeled brain structures was registered to the ex vivo average image to calculate the volume of brain structures in each image (15). This atlas was modified for the in vivo image analysis to contain 47 structures to accommodate the lower

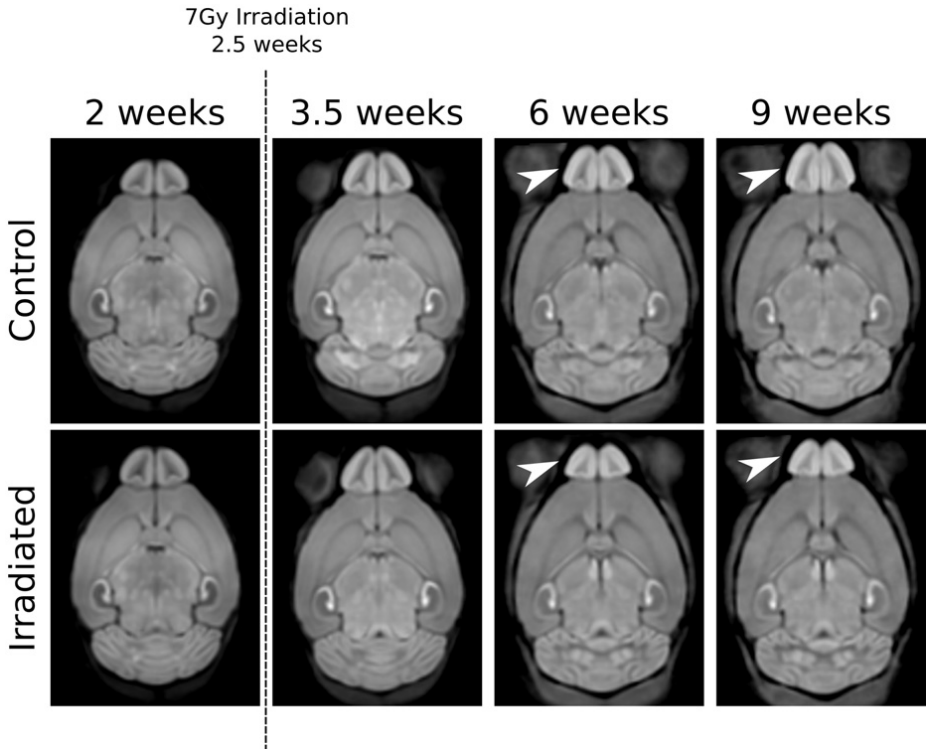

Fig. 1. Average manganese-enhanced magnetic resonance images of control and irradiated mice at different time points. The most apparent difference here is the smaller volume of the olfactory bulb in the irradiated group (arrowheads).

resolution and manganese-enhanced contrast (see Supplementary Fig. e1).

The longitudinal in vivo data were fit with a piecewise linear mixed effects model with a change-point at 3.5 weeks. Random intercepts for each mouse were included in the model to account for biological variability. Control and irradiated groups were allowed different early volume changes and growth rates after the first postirradiation time point. We performed statistical testing of the early volume changes (between 2 and 3.5 weeks of age) and long-term growth rates (the average rate between 3.5 and 9 weeks of age) between control and irradiated groups both voxelwise and structurewise, correcting for multiple comparisons using the false discovery rate (FDR) as previously described, assuming independent tests (16).

For the 6-week ex vivo data, statistical comparisons between control and irradiated groups were made using a *t* test. Again, volume differences were tested voxelwise and structurewise, with statistical thresholding using the FDR.

Histopathology and immunohistochemistry

Three control and 3 irradiated brains were evaluated histologically at each of the 6- and the 9-week time points. Hematoxylin and eosin (H&E) staining of 4-μm-thick sections was performed using standard methods. Sections (20 μm) were immunostained using free-floating methods. Briefly, sections were incubated at 4°C overnight with rabbit polyclonal anti-doublecortin (1:1000, Abcam) or mouse immunoglobulin (Ig)G anti-myelin basic protein (1:500, Millipore) primary antibodies, followed by 2 hours at room temperature with Cy3-conjugated AffiniPure donkey anti-rabbit IgG or donkey anti-mouse IgM secondary antibodies (1:100 Jackson ImmunoResearch), respectively. Antibodies were diluted in antibody diluent buffer (Dako), and sections were counterstained with 4′6-diamidino-2-phenylindole.

Results

Irradiation causes early volume deficits in many brain regions and a reduced long-term growth rate in the olfactory bulb

Longitudinal evaluation of mouse brain development following whole-brain irradiation at 2.5 weeks of age revealed developmental impairment throughout much of the brain. Representative slices from average images produced for each imaging time point are provided in Fig. 1. We evaluated these images on a voxel-by-voxel basis for (*1*) an early volume difference between 2 and 3.5 weeks of age and (*2*) a long-term growth rate difference obtained from all postirradiation time points. On a voxel-by-voxel comparison, many brain regions experienced an initial volume deficit in irradiated brains relative to controls followed by growth at a normal rate, remaining persistently smaller through the developmental time points observed (Fig. 2A and 2C). Regions in the olfactory bulb showed a slower long-term growth rate, resulting in a progressive volume deficit following irradiation (Fig. 2B and 2D).

Additional evaluation of brain development based on segmented structure volumes also revealed altered development in irradiated mice (Fig. 3). Twenty-one of the 47 segmented structures, a subset of which is plotted in Fig. 3, as well as the whole brain, showed an early volume deficit of 2%-8% at 3.5 weeks of

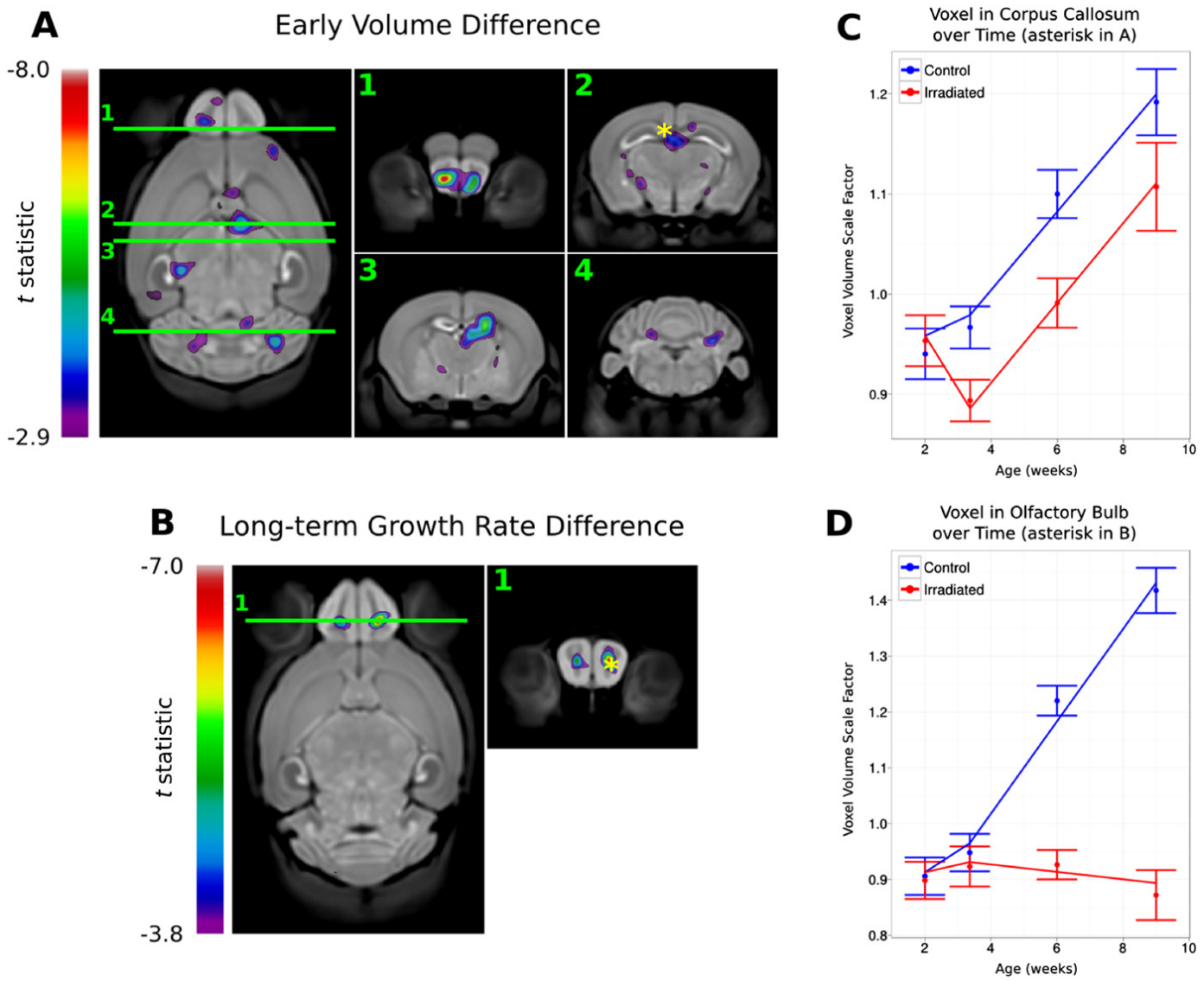

Fig. 2. Voxelwise comparison of brain development in irradiated and control mice (A) Average in vivo image overlaid with color maps indicating regions that experience an early volume deficit as indicated by a significantly smaller volume at 3.5 weeks (10% false discovery rate; greater significance indicated by hot colors). Significant differences were seen in regions including the corpus callosum (2), olfactory bulb (1), hippocampus (3), and cerebellum (4). (B) Average in vivo image overlaid with color maps indicating regions with significantly slower growth after the first postirradiation time point. Although these regions may not show an early volume deficit, the significantly slower long-term growth rate produces a progressive defect. (C,D) The volume of voxels indicated by asterisks in the corpus callosum and olfactory bulb shown over time. The vertical axis shows the value of the Jacobian determinant, representing a volume scale factor relative to the volume in the average image. The plots give an indication of the growth differences illustrated in panels A and B. Error bars represent standard error.

age in irradiated mice compared with controls (5% FDR; see also Supplementary Table e1). Following the initial volume deficit, the majority of the structures affected grew at a normal rate, remaining smaller at all time points. As a result, these structures in the irradiated mice required an average of 13 days (SD 5 days) longer to attain the same volumes as in control mice at the 3.5-week time point. The olfactory bulb showed a progressive volume deficit, exhibiting a 7% smaller volume at 3.5 weeks in the irradiated mice and then growing at less than half the rate of the control mice. This resulted in a 35-day delay for this structure in the irradiated brains to reach the 3.5-week control volume and in a 15% smaller volume at the final 9-week time point. Long-term growth rate comparisons for all structures are provided in Supplementary Table e2. For some structures, the difference at the 6-week time point was actually larger than at either the 3.5- or 9-week time points. Although this trend would be more accurately modeled by more complex growth curves, given the number of time points examined, we elected to use a simple linear model here.

Irradiated brains are smaller in both white matter and gray matter regions 3.5 weeks after irradiation

Higher resolution and better contrast is obtained with ex vivo imaging. We therefore evaluated volume differences at 6 weeks

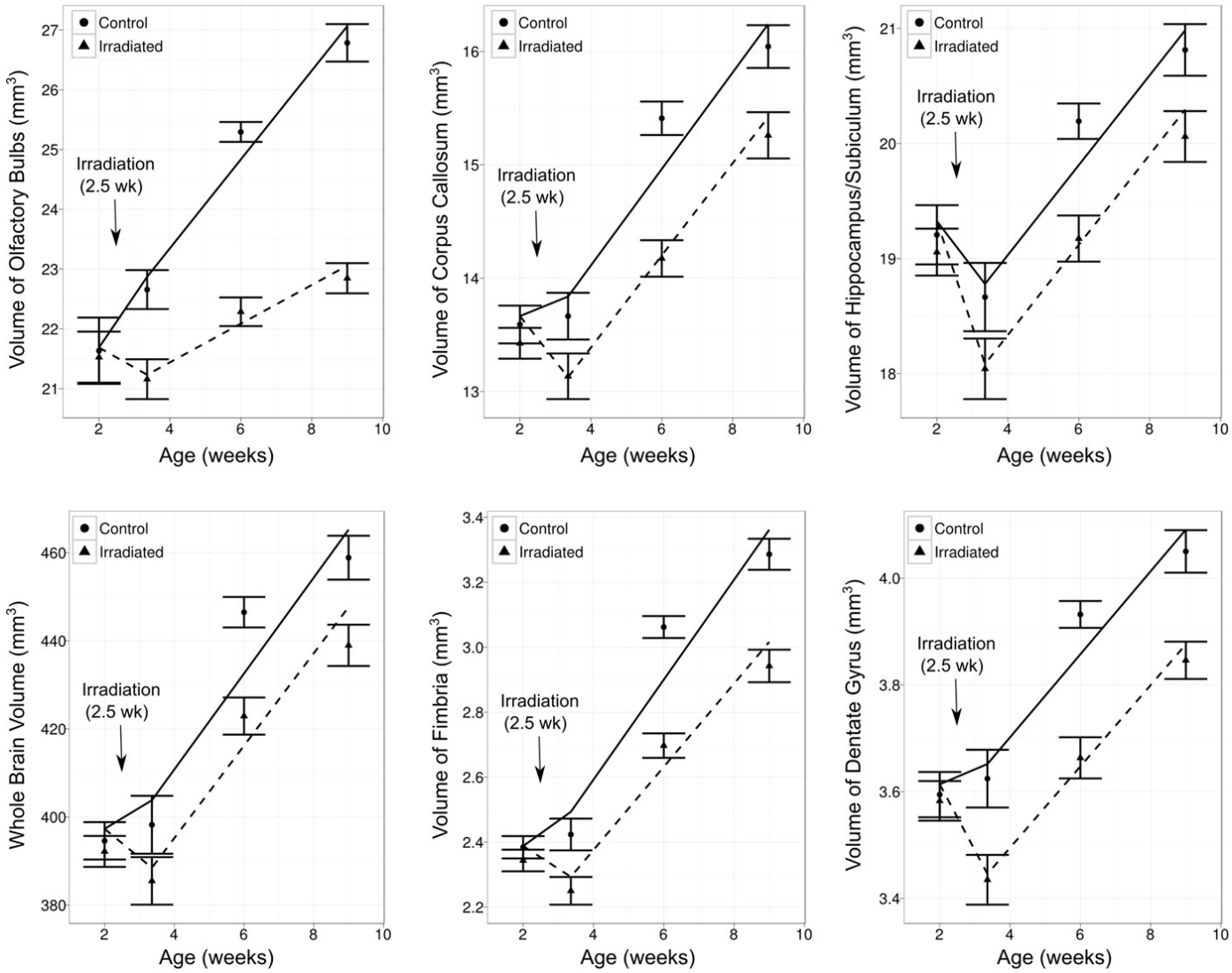

Fig. 3. Evaluation of brain development by structure following irradiation. Plots show the growth of selected structures over time. The olfactory bulb shows an early and progressive injury, with a significantly smaller volume at 3.5 weeks and a slower growth rate thereafter. The majority of affected structures, including the dentate gyrus, fimbria, corpus callosum, hippocampus, and the whole brain shown here, show an early deficit, with smaller volumes at 3.5 weeks, followed by normal average growth. Error bars represent standard error.

of age voxelwise and structurewise in ex vivo samples after irradiation at 2.5 weeks. As a comparison, we also evaluated the 6-week in vivo images independently for volumetric differences, providing a simple control for possible influences of multiple $MnCl_2$ injections and imaging sessions. Based on visual inspection of the voxelwise data, the ex vivo data show much of the same results as volumetric analyses of the 6-week in vivo data, with somewhat larger regions of significance (Fig. 4).

As seen in the longitudinal study, a large number of brain structures, as well as the whole brain, were significantly smaller in irradiated mice compared with controls at 6 weeks of age (Fig. 5). After grouping predominantly white and gray matter structures, it was clear that both total white matter and total gray matter volumes were significantly decreased in the irradiated brains by 10% and 5%, respectively. As gray matter accounts for a much larger fraction of the whole-brain volume than white matter in mice, loss in gray matter accounted for most of the 6% overall decrease in brain size (Fig. 5A, whole brain).

Histological evaluation reveals demyelination and loss of neural progenitor cells

Histological differences were evident in the irradiated brains at 6 and 9 weeks of age in regions where volume differences were observed on MRI. Evidence of changes in white matter and the subgranular zone were visible in the irradiated brains with H&E staining (Fig. 6A-6F). Doublecortin staining in the subgranular zone of irradiated mice revealed a substantial loss of neural progenitor cells (Fig. 6G-J). The irradiated brains also showed decreased myelin basic protein staining, suggesting a loss of myelin in white matter regions (Figure 6K-6N) consistent with previous reports (17).

Discussion

An estimated two-thirds of childhood cancer survivors experience late effects after cancer therapy (2), and neurocognitive late

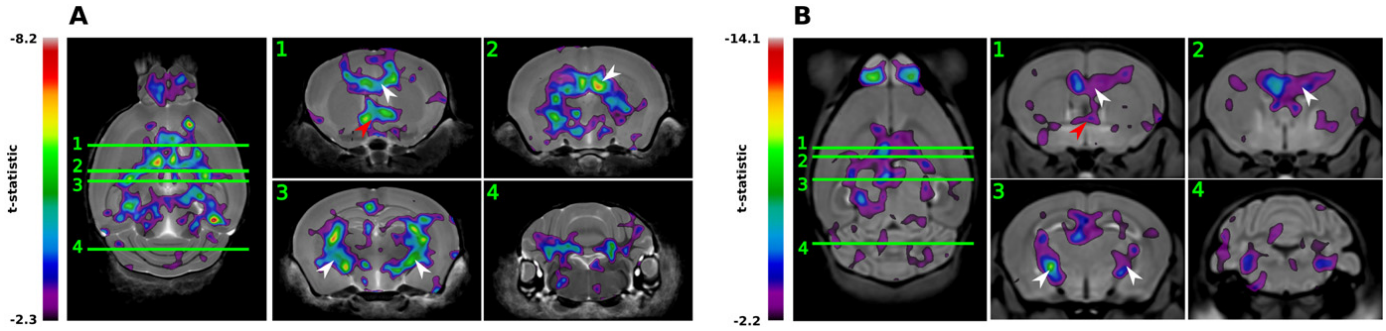

Fig. 4. Voxelwise volume comparison at 6 weeks of age. (A,B) Average (A) ex vivo and (B) in vivo images overlaid with color maps indicating regions that are significantly smaller in irradiated mice at 6 weeks of age (5% false discovery rate; higher significance indicated by hot colors). Qualitatively, the affected regions, specifically the corpus callosum (white arrowheads in 1), anterior commissure (red arrowheads in 1), fimbria (arrowheads in 2), and cerebral peduncles (arrowheads in 3), are common to the ex vivo and equivalent in vivo images.

effects have been linked to the use of cranial radiation therapy. Reduction of delivered dose and conformal radiation therapy are options being explored in the hope of reducing the occurrence of late effects (18). This study characterized the radiation response of structures throughout the mouse brain after irradiation at 2.5 weeks of age.

Our MRI and histology results are consistent with previously published work (19, 20) and provide an additional spatiotemporal map of radiation-induced developmental changes. We observed radiation-induced loss of white matter volume on MRI associated with demyelination seen histologically. We also found many gray matter regions to be affected, leading to a significant reduction in overall brain volume in irradiated animals. Cell loss within the neurogenic niches of subgranular zone of the dentate gyrus and subventricular zone was apparent histologically. We consider it unlikely that the imaging sessions and manganese injections have significantly influenced the longitudinal time course because qualitative comparison of in vivo vs ex vivo maps at the 6-week time point suggest only small differences.

The long-term growth rate (after irradiation and through to adulthood) for most brain structures did not appear to be significantly impaired. Rather, the majority of affected brain regions demonstrated an early volume deficit relative to controls followed by growth at a normal rate. This resulted in persistently smaller volumes throughout development. It will be important to determine whether short-term intervention soon after treatment can

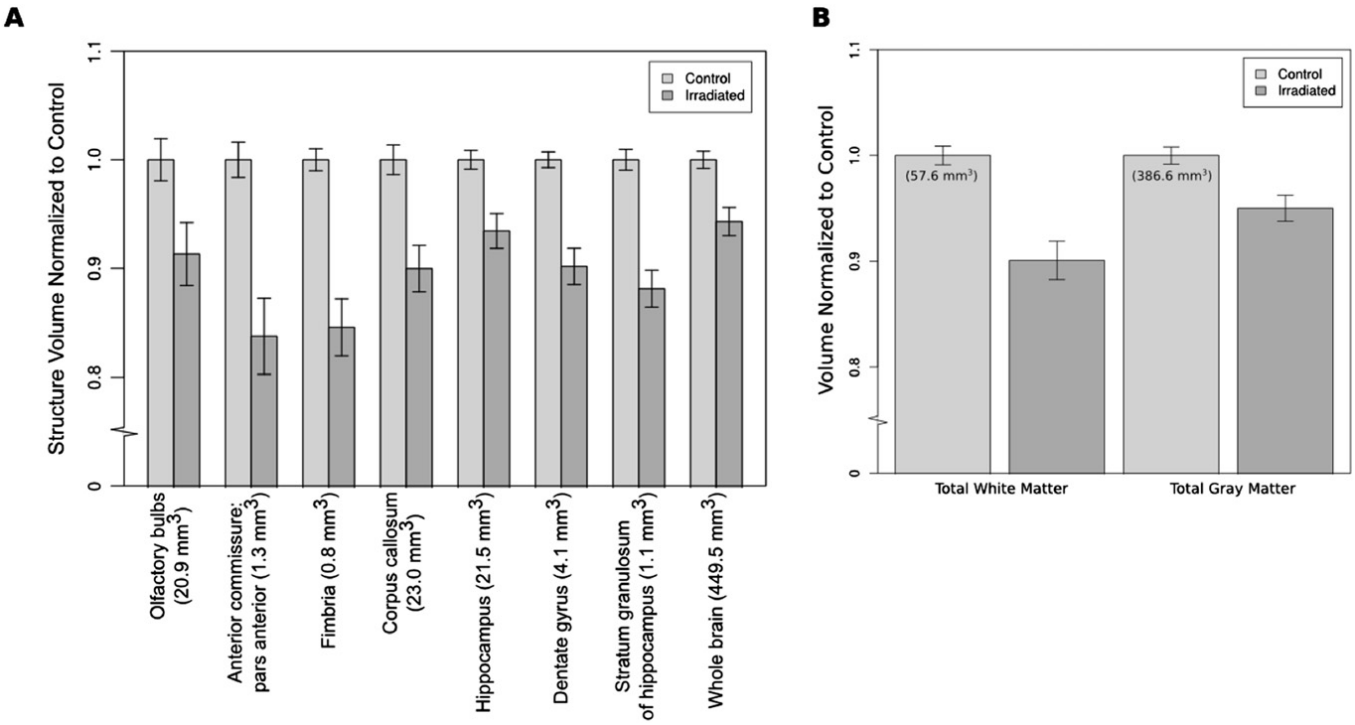

Fig. 5. Comparison of brain structure volume between control and irradiated mice at 6 weeks of age (ex vivo). (A) Volumes (normalized to control volumes indicated in brackets) of a subset of the structures that are smaller in the irradiated mice (5% false discovery rate). (B) Total white matter and gray matter volumes in control and irradiated mice, normalized to control. Similarly to the in vivo results, the effect of the irradiation is widespread and is seen in both white and gray matter structures. Although both white and gray matter volume is reduced in irradiated mice ($P<.001$), the white matter volume reduction is more severe (10% reduction in white matter vs 5% reduction in gray matter).

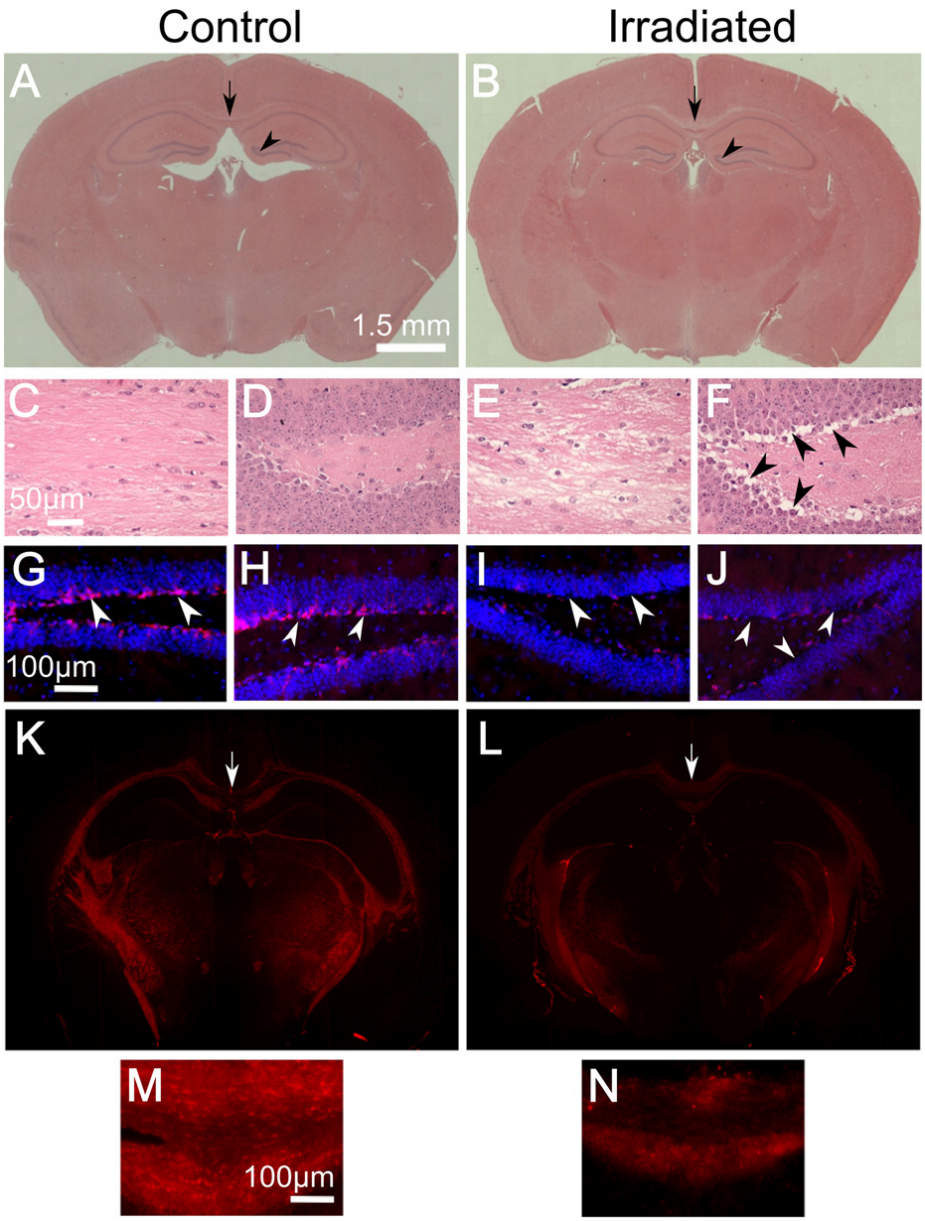

Fig. 6. Demyelination and loss of immature neurons in the mouse brain after irradiation. Compared with controls (A), irradiated brains (B) showed structural changes on hematoxylin and eosin-stained sections consistent with demyelination in the corpus callosum (arrows in A and B; shown at higher magnification in C and E) and cell loss in the dentate gyrus (arrowheads in A and B; higher magnification in D and F). In the dentate gyrus, doublecortin (DCX) staining showed a marked reduction in immature neurons in the subgranular zone of the irradiated brain (arrowheads; G and H, control; I and J, irradiated; blue, 4′6-diamidino-2-phenylindole; red, DCX). Loss of myelin basic protein (K, control; L, irradiated) staining in white matter is also consistent with demyelination. This is apparent in the corpus callosum at high power (M, control; N, irradiated; from the region indicated by arrows in K and L).

normalize volume outcomes by eliminating the early volume change in these structures and to assess further whether this also alleviates late effect symptoms.

Conversely, we observed that the olfactory bulb experienced prolonged growth impairment. The olfactory bulb is a structure that relies on a continuous supply of neural progenitor cells to maintain its neuronal population, and damage to this cell population likely contributed to its impaired development. The dentate gyrus is a site of neurogenesis in the adult brain. Although we did not see a progressive growth deficit in this structure, it did show an early volume deficit that persisted throughout the study. This effect may be related to the learning deficits experienced by childhood brain cancer survivors.

This study characterized how irradiation at a young age affects brain development. Normalization of this time course is expected to be critical to eliminating radiation-induced late effects. A longer-term study may reveal that some affected structures show partial recovery, which might serve to further identify delayed vs permanently impaired developmental processes. Additional investigation of which volume changes are most tightly linked with behavioral symptoms in mice will help prioritize anatomical targets for intervention.

The imaging methods used in this study are highly sensitive to radiation-induced anatomic changes in the developing mouse brain. The ability to study the whole brain over time after irradiation may aid in investigating neuroprotective strategies

intended to mitigate late effects and may reveal macroscopic changes to guide investigation of the underlying mechanisms that lead to these effects. Furthermore, these methods can be readily applied to the study of transgenic mouse models, which may be valuable tools for elucidating the cellular mechanisms underlying the observed CNS response to radiation.

References

1. US Cancer Statistics Working Group. United States Cancer Statistics: 1999-2007 Incidence and Mortality Web-based Report. Centers for Disease Control and Prevention Web Site. www.cdc.gov/uscs. 2010. Accessed February 17, 2012.
2. Landier W, Bhatia S. Cancer survivorship: A pediatric perspective. *Oncologist* 2008;13:1181-1192.
3. Anderson DM, Rennie KM, Ziegler RS, et al. Medical and neurocognitive late effects among survivors of childhood central nervous system tumors. *Cancer* 2001;92:2709-2719.
4. Johnston DL, Keene D, Bartels U, et al. Medulloblastoma in children under the age of three years: A retrospective Canadian review. *J Neurooncol* 2009;94:51-56.
5. Ellenberg L, Liu Q, Gioia G, et al. Neurocognitive status in long-term survivors of childhood CNS malignancies: A report from the Childhood Cancer Survivor Study. *Neuropsychology* 2009;23:705-717.
6. Mulhern RK, Palmer SL. Neurocognitive late effects in pediatric cancer. *Curr Probl Cancer* 2003;27:177-197.
7. Grundy RG, Wilne SA, Weston CL, et al. Primary postoperative chemotherapy without radiotherapy for intracranial ependymoma in children: The UKCCSG/SIOP prospective study. *Lancet Oncol* 2007;8:696-705.
8. Tofilon PJ, Fike JR. The radioresponse of the central nervous system: A dynamic process. *Radiat Res* 2000;153:357-370.
9. Wong CS, Van der Kogel AJ. Mechanisms of radiation injury to the central nervous system: implications for neuroprotection. *Mol Interv* 2004;4:273-284.
10. Fike JR, Rosi S, Limoli CL. Neural precursor cells and central nervous system radiation sensitivity. *Semin Radiat Oncol* 2009;19:122-132.
11. Mabbott DJ, Noseworthy MD, Bouffet E, et al. Diffusion tensor imaging of white matter after cranial radiation in children for medulloblastoma: Correlation with IQ. *Neuro Oncol* 2006;8:244-252.
12. Clancy B, Darlington RB, Finlay BL. Translating developmental time across mammalian species. *Neuroscience* 2001;105:7-17.
13. Wadghiri YZ, Blind JA, Duan X, et al. Manganese-enhanced magnetic resonance imaging (MEMRI) of mouse brain development. *NMR Biomed* 2004;17:613-619.
14. Lerch JP, Sled JG, Henkelman RM. MRI phenotyping of genetically altered mice. *Methods Mol Biol* 2011;711:349-361.
15. Dorr AE, Lerch JP, Spring S, et al. High resolution three-dimensional brain atlas using an average magnetic resonance image of 40 adult C57Bl/6J mice. *Neuroimage* 2008;42:60-69.
16. Genovese CR, Lazar NA, Nichols T. Thresholding of statistical maps in functional neuroimaging using the false discovery rate. *Neuroimage* 2002;15:870-878.
17. Kurita H, Kawahara N, Asai A, et al. Radiation-induced apoptosis of oligodendrocytes in the adult rat brain. *Neurol Res* 2001;23:869-874.
18. Packer RJ, Gajjar A, Vezina G, et al. Phase III study of craniospinal radiation therapy followed by adjuvant chemotherapy for newly diagnosed average-risk medulloblastoma. *J Clin Oncol* 2006;24:4202-4208.
19. Mulhern RK, Reddick WE, Palmer SL, et al. Neurocognitive deficits in medulloblastoma survivors and white matter loss. *Ann Neurol* 1999;46:834-841.
20. Reddick WE, Russell JM, Glass JO, et al. Subtle white matter volume differences in children treated for medulloblastoma with conventional or reduced dose craniospinal irradiation. *Magn Reson Imaging* 2000;18:787-793.